Porous PDMS-Based Microsystem (ExoSponge) for Rapid Cost-Effective Tumor Extracellular Vesicle Isolation and Mass Spectrometry-Based Metabolic Biomarker Screening

Joseph Marvar, Abha Kumari, Nna-Emeka Onukwugha, Abhinav Achreja, Noah Meurs, Olamide Animasahun, Jyotirmoy Roy, Miya Paserba, Kruthi Srinivasa Raju, Shawn Fortna, Nithya Ramnath, Deepak Nagrath, Yoon-Tae Kang,* and Sunitha Nagrath*

Polydimethylsiloxane (PDMS) is an inexpensive robust polymer that is commonly used as the fundamental fabrication material for soft-lithography-based microfluidic devices. Owing to its versatile material properties, there are some attempts to use PDMS as a porous 3D structure for sensing. However, reliable and easy fabrication has been challenging along with the inherent hydrophobic nature of PDMS hindering its use in biomedical sensing applications. Herein, a cleanroom-free inexpensive method to create 3D porous PDMS structures, "ExoSponge" and the effective surface modification to functionalize its 3D porous structure is reported. The ability of ExoSponge to recover cancer-associated extracellular vesicles (EVs) from complex biological samples of up to 10 mL in volume is demonstrated. When compared to ultracentrifugation, the ExoSponge shows a significant increase in cancer EV isolation of more than 210%. Targeted ultra-high pressure liquid chromatography-tandem mass spectrometry (LC-MS/MS) is further employed to profile 70 metabolites in the EVs recovered from the lung cancer patient's plasma. The resulting profiles reveal the potential intraexosomal metabolite biomarker, phenylacetylglutamine (PAG), in non-small cell lung cancer. The high sensitivity, simple usage, and cost-effectiveness of the ExoSponge platform creates huge potential for rapid, economical and yet specific isolation of exosomes enabling future diagnostic applications of EVs in cancers.

1. Introduction

Extracellular vesicles (EVs) are naturally secreted membrane-bound nanovesicles from cells that are involved in intercellular communication. Their membrane contains and protects proteins, nucleic acids, and metabolites. Hence, they can serve as active cargo delivery vehicles and messengers of genetic information.[1] There has been an increased interest in the clinical use of EVs as biomarkers due to their significance in cellular signaling, disease progression, and therapeutics. The isolation and characterization of exosomes allow their use as reliable biomarkers for minimally invasive disease diagnosis, called liquid biopsy. One of the promising opportunities for disease diagnosis is the diagnosis of cancer since EV secretion is increased by many cancer types. Their presence in a variety of biosamples – that is, blood, urine, saliva – makes them an attractive avenue for exploration for liquid biopsy to provide a simple, in vitro analysis of a patient's tumor status.[2,3] Deregulated cellular metabolism has been established as a hallmark of cancer which supports the use of metabolite characterization as a sensitive, inexpensive, and origin-agnostic tool for minimally-invasive diagnosis of cancer.[4] However, the large amounts of biosample contaminants and the size of the desired endosome-derived small EVs (sEV), also called exosomes, at just 30–150 nm diameter makes isolation difficult and challenging[5] using conventional EV isolation methods.

J. Marvar, A. Kumari, N.-E. Onukwugha, K. S. Raju, D. Nagrath, Y.-T. Kang, S. Nagrath
Department of Chemical Engineering and Biointerfaces Institute
University of Michigan
2800 Plymouth Road, NCRC B10-A184, Ann Arbor, MI 48109, USA
E-mail: kyoontae@umich.edu; snagrath@umich.edu
A. Achreja, N. Meurs, O. Animasahun, J. Roy, M. Paserba, D. Nagrath
Department of Biomedical Engineering
University of Michigan
Carl A. Gerstacker Building, 2200 Bonisteel Blvd
Ann Arbor, MI 48109, USA

The ORCID identification number(s) for the author(s) of this article can be found under https://doi.org/10.1002/admt.202201937.

S. Fortna
Department of Mechanical Engineering
University of Michigan
G.G. Brown Laboratory
2350 Hayward, Ann Arbor, MI 48109, USA
N. Ramnath
Department of Internal Medicine
University of Michigan
Ann Arbor, MI 48109, USA
S. Nagrath
Rogel Cancer Center
University of Michigan
1500 E Medical Center Dr., Ann Arbor, MI 48109, USA

**ADVANCED
SCIENCE NEWS**

www.advancedsciencenews.com

**ADVANCED
MATERIALS
TECHNOLOGIES**

www.advmattechnol.de

Ultracentrifugation (UC) is the primary practice used for EV isolation being considered the "gold standard". However, UC requires expensive machinery, large operating dilution ratios, and a long procedure time which makes small or mid-bulk volume (100 µl–5 ml) sample isolation impractical. Other techniques such as the use of magnetic bead kits and polyethylene glycol (PEG) have been effective with minimal volume samples but magnetic bead kits can only accommodate low sample throughput and PEG has low EV specificity due to its principle of settling all small-sized particles during processing. Even when only obtaining low purity yields, a bulk sample of just several milliliters would be too expensive for PEG, with prices of $100 per test when scaling up.[6] Recent works using methacrylate-based monolithic disc columns utilize selective immunoaffinity-based isolation of platelet-derived EVs from plasma.[7,8] However, poor yields and the inability to isolate a specific subpopulation of EVs limit their applications in downstream analysis for clinical studies.

Microfluidic approaches have shown superior specificity and high-throughput performance for samples up to sub milliliter in volume,[9–11] however, it is not cost-effective when it comes to processing mid-bulk volume samples (1–10 ml), which is often needed for genomics/metabolomics studies with enough sample quantities to be detected. Their bulk isolation ability is limited by their total sample processing volume per device that usually handles sub-microliter samples. Thus, technologies that can isolate EVs from mid-bulk samples at lower costs and high yields are urgently needed. Some recent attempts towards this topic include ExoTic, a size-based isolation chip that produces high yield and purity of isolated EVs from low to high volumes of samples.[12] However, it can be limited by filter clogging issues as well as pump stalling with flow rates higher than 5 ml per hour for small pore-size filters. Additionally, our group recently devised a liquid biopsy hydrogel platform, ExoBeads, for easily scaling up antibody-based EV isolation for larger volume samples.[13] Here, we present our new PDMS-based quick EV isolation platform, ExoSponge, which is cheaper and has easier sample handling when compared to ExoBeads.

Polydimethylsiloxane (PDMS) is commonly used to fabricate cheap, robust, and high-resolution microfluidic systems in the fields of biology and medicine such as microfluidic devices, microreactors, and microchannels for electrophoresis.[14,15] There have also been attempts to utilize PDMS's versatile properties to construct porous 3D structures, such as the porous microneedles developed by Takeuchi et al. for non-invasive healthcare monitoring.[16] However, previous studies describe the diverse application of the PDMS structures ranging from pressure sensing to the use of protective layers for robotics.[17–20] Furthermore, the inherent hydrophobic nature of PDMS makes the manipulation of elements in aqueous solutions ineffective and impractical such that there have not been attempts to combine PDMS porous 3D structure with its biocompatible potential. As a result, previous works discussed various fabrication technologies for 3D porous PDMS platforms but with limited biological applications.[21,22] Here, we present a unique yet simple fabrication method to create the 3D porous PDMS sponge-like structure. Our method uses simple sugar cubes for creating the porous structures and does not require any cleanroom processing to create a bio-functional 3D porous structure. We describe a chemical treatment approach that oxidizes its large surface area making it optimal for its use with biosamples.

Utilizing the hydrophilicity of oxidized PDMS along with the high surface area characteristics of the porous 3D structure, we can create a suitable scaffolding for immuno/lipid-affinity-based biomarker isolation, such as EVs. With additional functionalization and target-capturing molecule conjugation, our porous PDMS platform, ExoSponge, can selectively target exosomes to isolate them from bulk samples of up to 5–10 mL (**Figure 1**). Previously, a highly sensitive method of isolation of exosomes with a limit of detection of 2.9×10^8 exosomes/ml was achieved using an anti-CD63-based immunoassay.[23]
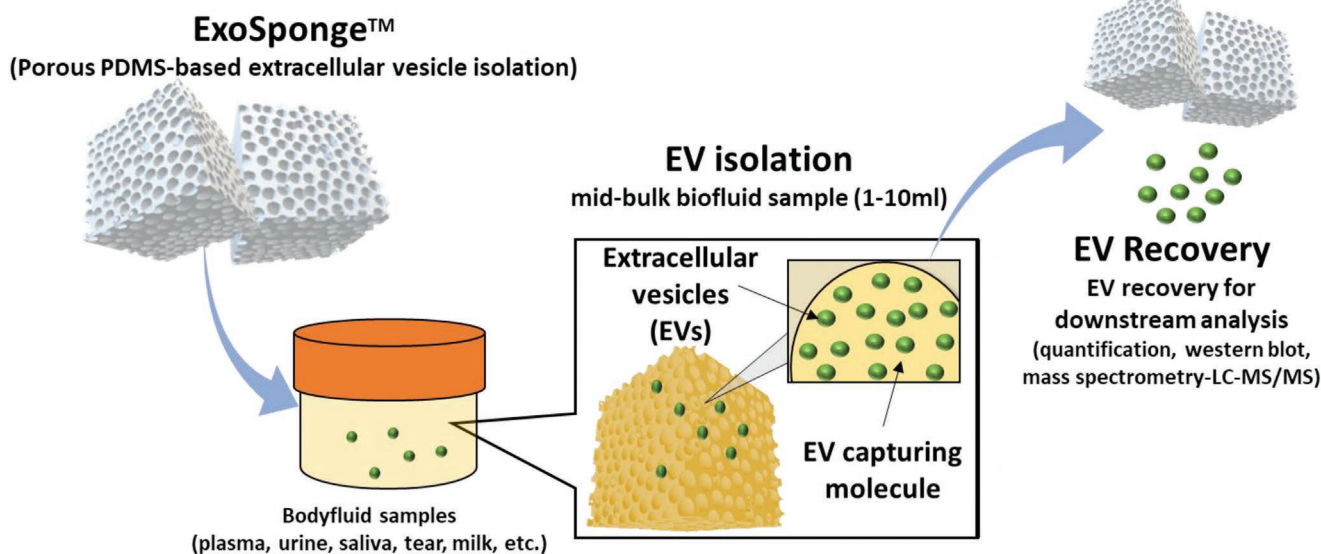
Figure 1. Porous polydimethylsiloxane (PDMS) based cancer-associated extracellular vesicle isolation and recovery from body fluid samples.

Similarly, Annexin V-based lipid affinity-based capture demonstrated the specific isolation of cancer-associated exosomes with an average capture efficiency of 90%.[24] Thus, our devices were conjugated with anti-CD63 antibodies to target the tetraspanin CD63 on exosomes and Annexin V for the specific capture of cancer-associated exosomes, respectively. To demonstrate the efficacy of this device, exosomes were isolated from serum samples of healthy and lung cancer patients using ExoSponge. The exosomes were further analyzed by liquid chromatography-tandem mass spectrometry (LC-MS/MS) followed by untargeted metabolomics to quantitatively profile the metabolite cargo of lung cancer exosomes. Previous EV isolation methods exacerbate the challenge of extracting metabolites at concentrations large enough to profile a broad range of polar metabolites. In addition, polar metabolite analysis from exosomes required over 5×10^{10} exosomes, obtainable from a culture of 15×10^{6} cells over 48 h.[25,26] While blood has a much higher concentration of exosomes at 10^{10}–10^{12} mL^{-1}, ultracentrifugation and solvent precipitation-based isolation techniques would still require at least 2–10 mL of blood plasma to provide an equivalent yield to that of ExoSponge.[27] Moreover, the ability to isolate and extract metabolites on the ExoSponge minimizes metabolite degradation and loss due to residual enzymatic activity and long procedures throughout the ultracentrifugation isolation and extraction steps.

Thus far, metabolic profiling of exosomes has been performed after extraction via ultracentrifugation or precipitation assays[26,28,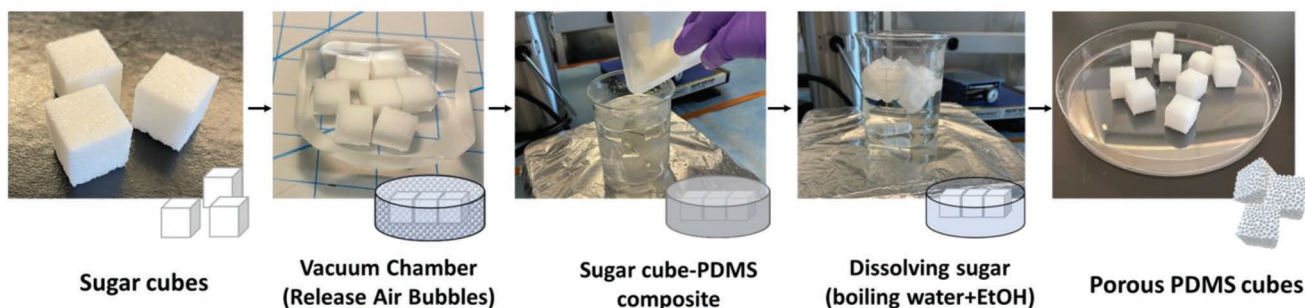29] and largely focused on lipidomics.[30–32] To the best of our knowledge, this is the first demonstration of a comprehensive study of small-molecule polar metabolites using a PDMS-based microsystem and our innovative porous PDMS scaffolding for affinity-based isolation can provide rapid, high-yield, and inexpensive EV isolation and profiling solution. These metabolites can be used to profile the metabolic state of the secreting cells through their soluble contents, providing an indication of the activity levels of a broad array of metabolic pathways. Due to the potent and diverse metabolic reprogramming of cancers, alterations in levels of polar metabolites contained within exosomes can serve as a simple, noninvasive readout for cancer diagnosis. Our results highlight the advantages of how the ExoSponge and the SCIEX 7500 UPLC-MS/MS can be uniquely integrated to overcome the challenges of broad metabolic profiling of extracellular vesicles.
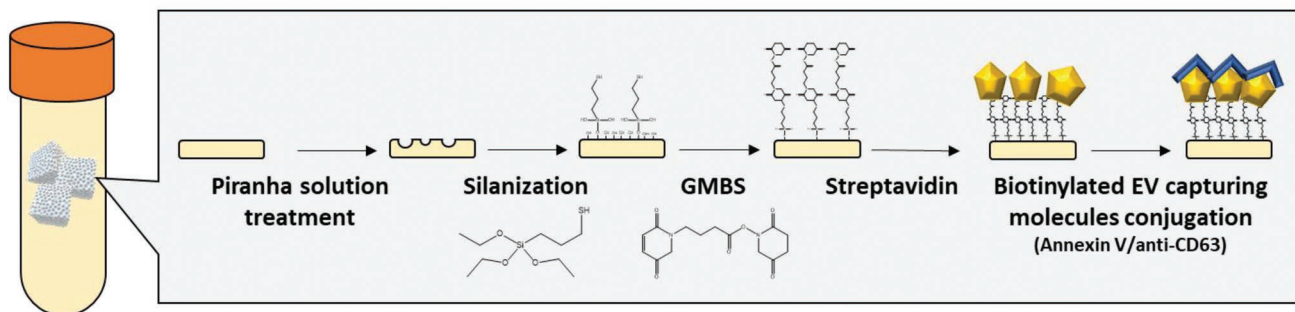
2. Results and Discussion

2.1. Cleanroom-Free Fabrication of Porous 3D PDMS Sponges

We have utilized commercially available widely used sugar cubes as a scaffold to make the porous PDMS sponges (**Figure 2**a). The sugar cubes were coated with a 10:1 PDMS pre-polymer and curing agent, then placed into a vacuum chamber for 40 min and subsequently placed in a 68 °C convection oven overnight for curing. To dissolve the sugar scaffold, the PDMS-coated sugar cubes were carefully cut out from

a. Porous PDMS fabrication

Sugar cubes → Vacuum Chamber (Release Air Bubbles) → Sugar cube-PDMS composite → Dissolving sugar (boiling water+EtOH) → Porous PDMS cubes

b. Surface modification of Porous PDMS

Piranha solution treatment → Silanization → GMBS → Streptavidin → Biotinylated EV capturing molecules conjugation (Annexin V/anti-CD63)

Figure 2. Fabrication and surface modification of porous PDMS cubes to isolate circulating biomarkers: a) Porous PDMS unit device created using sugar cube scaffold; Sugar cubes were submerged in PDMS solutions and then PDMS adsorbed sugar cubes were cured. Then the sugar is dissolved to reveal the porous PDMS 3D structures; b) surface modification of porous PDMS unit to isolate circulating biomarkers.

**ADVANCED
SCIENCE NEWS**
www.advancedsciencenews.com

**ADVANCED
MATERIALS
TECHNOLOGIES**
www.advmattechnol.de

their container and submerged into a beaker of 90 °C water for 1–2 h with constant stirring. The beakers were replaced with fresh water every 30 min to maximize sugar transport. Lastly, the PDMS-sugar cube devices were stored in a 70% ethanol beaker overnight and squeezed dry of excess ethanol upon functionalization.

2.2. Characterization of Porous PDMS

The porous PDMS structure creates a high-surface area device with the ability to be easily modified for functionalization (Figure 2b). The device inherits the micro-pores of the sugar scaffolding. Analysis of cross-sectional slices of the device showed the pore sizes are semi-consistent throughout with an average pore diameter of 408.9 µm ± 91.8 as shown in **Figure 3**a. The pore size frequency follows a normal distribution

(Figure 3a right). Also, the center slice diameters tend to be the largest with the pore sizes decreasing toward the surface of the device. This could be a result of the PDMS resin not being able to penetrate as effectively into the sugar cube's center as it would on the surface. The cross-sectional view of the porous PDMS cut is shown in Figure 3b. We further evaluated the compressibility/wettability of the ExoSponge which allows the device to release absorbed liquid such as biological samples (Figure 3c). After oxidation by piranha solution treatment, the device is transformed from the inherent hydrophobicity of PDMS to being hydrophilic. This not only increases the wettability of the device for aqueous solutions but also roughens the surface of the device for a higher binding chance between device and EVs.[33,34]

The porosities of the unfunctionalized device (72.7% ± 5.08%) and sugar cube scaffolding used (34.2% ± 1.14%) were measured along with the device after functionalization (57.9% ± 2.21%)
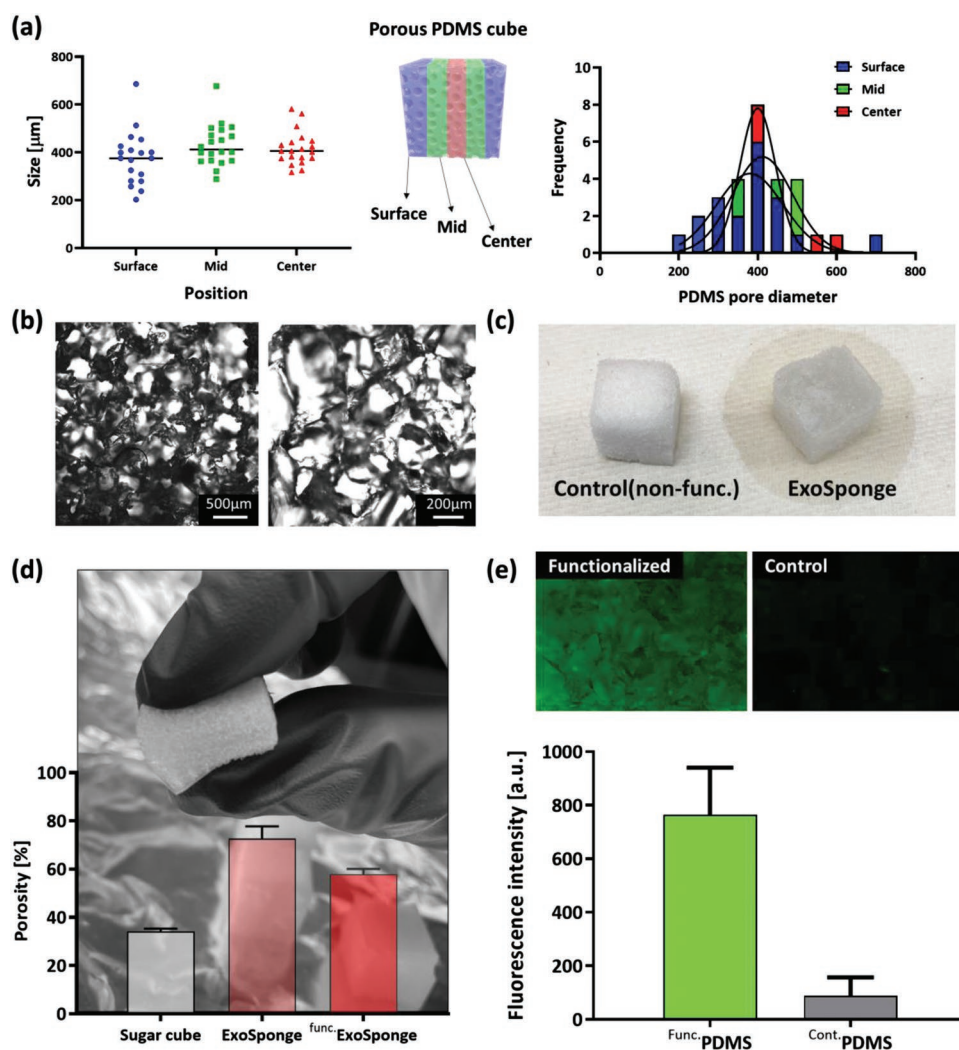
Figure 3. Evaluation of porous PDMS fabrication and functionalization: a) pore size evaluation at the surface, mid-center, and center (left), and pore size distribution at the three different locations (right); b) microscopic images of porous PDMS cube slices; c) evaluation of wettability in porous PDMS unit between pre-functionalization(hydrophobic) and post-functionalization(hydrophilic); d) porosity evaluation for sugar cube, porous PDMS unit and functionalized porous PDMS unit, ExoSponge; e) quantitative analysis of fluorescence intensities between avidin-functionalized device and control device after biotinylated fluorescence dye (top left) and its surface under fluorescence microscopy (top right).

(Figure 3d). Following silane-GMBS and NeutrAvidin conjugation, the devices were evaluated with biotinylated fluorescent dye to check whether the device was effectively conjugated with avidin. The results in Figure 3e show the avidin conjugation was successful yielding fluorescence intensities more than 7x the unmodified control porous PDMS.

2.3. Demonstration of EV Isolation using EV Capturing Molecule Conjugation

The Annexin V conjugation on the device will selectively bind to phosphatidylserine (PS) on cancer-derived extracellular vesicles in the presence of calcium ions while an anti-CD63 conjugated device will isolate general CD63 tetraspanin protein-expressing EVs that is common for exosome isolation (**Figure 4**a). This versatility will allow the ExoSponge device to isolate general EVs or specific subpopulations on demand in a sample based on the experiments. In Figure 4b, the scanning electron microscopy

(SEM) images show the capture of exosomes on the Annexin V-conjugated porous device's surface. Further, the Annexin V-conjugated device will eventually be subjected to an EDTA solution that will remove the calcium ions, disrupt the affinity, and release the isolated EVs.

2.4. EV Isolation/Release Performance using ExoSponge

The ExoSponge has been optimized concerning EV capturing molecules, optimal incubation time, device size, and external force during isolation. The optimization was evaluated in terms of total EV concentration, exosome-sized concentration, and purity of the samples. Exosome concentration was calculated from EVs in the size range of 30–150 nm and purity was determined as the fraction of isolated EVs that were exosomes. We first compared the EV capturing performance between Annexin V(Av) conjugated ExoSponge and anti-CD63 conjugated ExoSponge
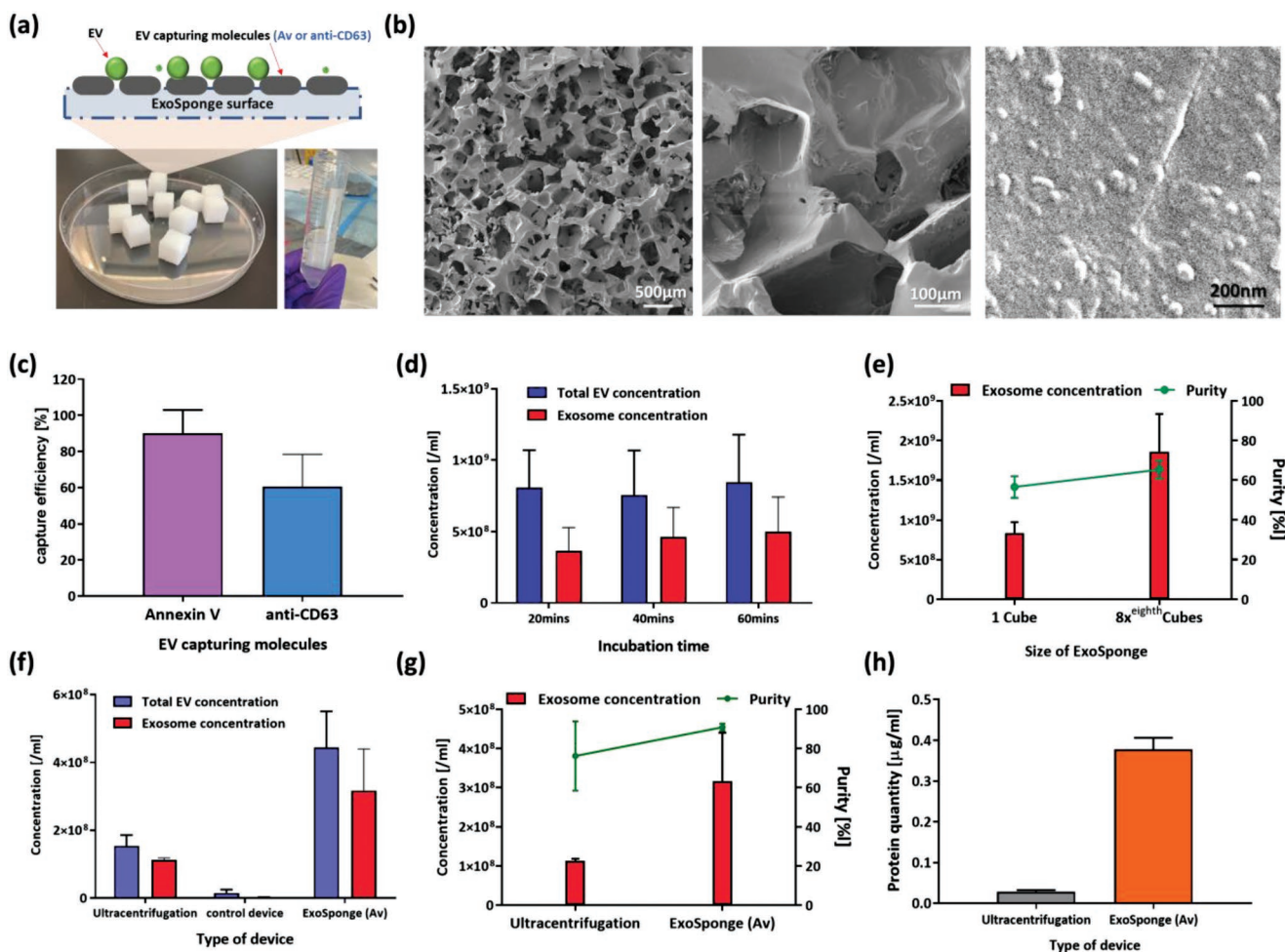
Figure 4. Cancer-associated extracellular vesicle (EV) isolation using porous PDMS cubes (ExoSponge) via Annexin V conjugation onto the device: a) fabricated and functionalized ExoSponge unit devices and working principle of extracellular vesicle isolation; b) scanning electron microscopy analysis of ExoSponge undergone EV isolation; c) EV capturing the performance of ExoSponge conjugated with Annexin V (Av) or anti-CD63; d) EV isolation performance depending incubation time with samples; e) exosome concentration comparison between 1 unit device and 8 × 1/8 unit devices; f–h) EV isolation comparison study with gold-standard extracellular vesicle isolation, ultracentrifugation, in terms of f) EV concentration, g) purity and exosome concentration, and h) total protein quantity.

**ADVANCED
SCIENCE NEWS**
www.advancedsciencenews.com

**ADVANCED
MATERIALS
TECHNOLOGIES**
www.advmattechnol.de

(Figure 4c). While anti-CD63 is a widely used exosome marker in immunoaffinity-based capture, the Av-conjugated ExoSponge captures 30% more lung cancer cell-derived exosomes (H3255) than anti-CD63-conjugated ExoSponge, which demonstrates cancer-associated EV isolation of Av-conjugated ExoSponge. The SEM images of ExoSponge with various EV capturing molecules showed similar results (Figure S1, Supporting Information)

The incubation time of ExoSponge with the sample was also optimized. After incubation trials of 20-, 40-, and 60-min periods, the exosome concentrations and total EV concentrations were recorded (Figure 4d). The results demonstrate a positive correlation between increased incubation time and increased exosome concentration. However, the 40-min period was determined optimal due to diminishing marginal gains as the incubation got longer. This allows for significant EV isolation while keeping the procedure time minimal.

The high surface area of the ExoSponge device might be responsible for its effective EV isolation. To analyze the effect of any further increase in surface area, the sugar cube template size was cut to decrease the volume to one-eighth of the original. The isolated sample's exosomal concentration and its purity were measured for both the original and smaller cube sizes, with the total device volume constant for each trial. Figure 4e shows that eight smaller cubes outperformed the original with an exosome concentration of 1.86×10^9 EVs mL^{-1} while the original cube only produced 8.36×10^8 EVs ml^{-1}. In addition, the purity also increased from 56.5% to 65.3% for the smaller cubes. However, the increased surface area of the smaller devices makes the total adsorbed volume increase from 1.9 mL per cube to 2.6 mL for the smaller cubes. This makes the EV concentrations similar regardless of device size. For this reason and that the smaller cubes make manipulation more difficult, the standard sugar cube size was chosen.

In attempts to reach higher isolation concentrations, the cubes were subjected to additional mechanical agitation from centrifugation (1000 rpm for 10 min) during incubation. For this optimization experiment, the devices were separated with half being subjected to centrifugation during its incubation while the rest were kept on a rocker. In Figure S2, Supporting Information, the presence of the external centrifugal force had no significant effect on the EV isolation concentration. The rocker incubation method was selected to keep the procedure simple.

2.5. EV Recovery Comparison Study

The ExoSponge device's isolation was compared to the gold-standard isolation method, ultracentrifugation (UC), as well as a porous PDMS device without capturing molecule conjugation. Using Nanoparticle tracking analysis (NTA), the ExoSponge device outperformed both methods in the total number of isolated EVs and its resulting sample exosome concentration when conjugated with anti-CD63 and Annexin V (Figure 4f and Figure S3, Supporting Information). Even with the higher measured exosome concentration, the ExoSponge device has no significant drop in the isolated sample purity when

compared to UC. Figure 4g shows UC with mean sample purity at $76.5 \pm 17.7\%$ and ExoSponge sample resulting in a purity of $90.9 \pm 1.83\%$ when functionalized with Annexin V, which shows greater exosome specificity using the ExoSponge device. This is as expected and proves the reliability of our porous PDMS platform regardless of the choice of antibody used for isolation. Additionally, in Figure 4h, micro-bicinchoninic acid (micro-BCA) protein analysis of the isolated exosomes also demonstrates ExoSponge as the more effective bulk isolation method when compared to UC. Western blot analysis of the recovered exosomes profiled proteins commonly found in cancer-derived EVs. These results show the ExoSponge device is a significantly more effective isolation method for bulk samples even when compared to the previous gold standard procedure.

2.6. Exosome Isolation from Plasma Samples Collected from Lung Cancer Patients

After analysis of the cell culture supernatant, we validated our device to study clinical specimens using patient plasma samples. We collected a plasma sample volume of 10 mL and used ExoSponge to isolate EVs as described in the Experimental Section. Subsequent to the capture of EVs, they are released from the ExoSponge and analyzed by NTA. NTA displayed successful EV isolation from both healthy and lung cancer samples and the ExoSponge device continued to outperform UC (**Figure 5**a) as well as more exosome-sized vesicle distribution (Figure 5b) For the lung cancer patient samples, ExoSponge yielded an average exosome isolation of 9.40×10^9 EV mL^{-1} while only 3.26×10^9 EV mL^{-1} for UC. In the healthy donor sample, ExoSponge and UC resulted in 2.64×10^9 and 2.23×10^9 EV mL^{-1}, respectively (Figure 5a-left). The smaller isolation difference in healthy donor cells could be a result of healthy cells not expressing much PS in comparison to cancer cells. We further quantified the total protein of the EVs isolated using both methods. As shown in Figure 5a-right, BCA analysis draws the same conclusion with ExoSponge having a protein quantity of 732.3 ± 10.6 µg mL^{-1} and UC with only 81.1 ± 34.0 µg mL^{-1}. The purity of the NTA isolated exosome sample was evaluated by the ratio of EV sized over all particles measured in solution. This analysis indicates that, unlike UC, ExoSponge has a higher purity for its cancer patient samples when compared to the healthy.

The surface of the functionalized ExoSponge device was mapped using an SEM after biosample exposure but before it was subjected to EDTA treatment to release exosomes. The SEM images show the porous 3D structure of the device and as the magnification was increased, EV-sized clusters (30–150 µm) appeared on the surface of the device providing visual evidence for successful exosome capture (Figure 5c). The results from 4 different clinical samples showed housekeeping protein, GAPDH, and exosomal marker CD63 expression (Figure 5d).

Further analysis of more blood plasma samples showed preferential isolation of exosomes derived from cancer patients in comparison to healthy ones (Figure 5e). ExoSponge yielded a mean exosome isolation concentration of $2.46 \times 10^9 \pm 7.31 \times 10^8$ EVs mL^{-1} for the healthy donor samples and $6.36 \times 10^9 \pm 5.03 \times 10^9$ EVs mL^{-1} for the lung cancer patients (Figure 5f). Previous research has highlighted the possible preference of Annexin V
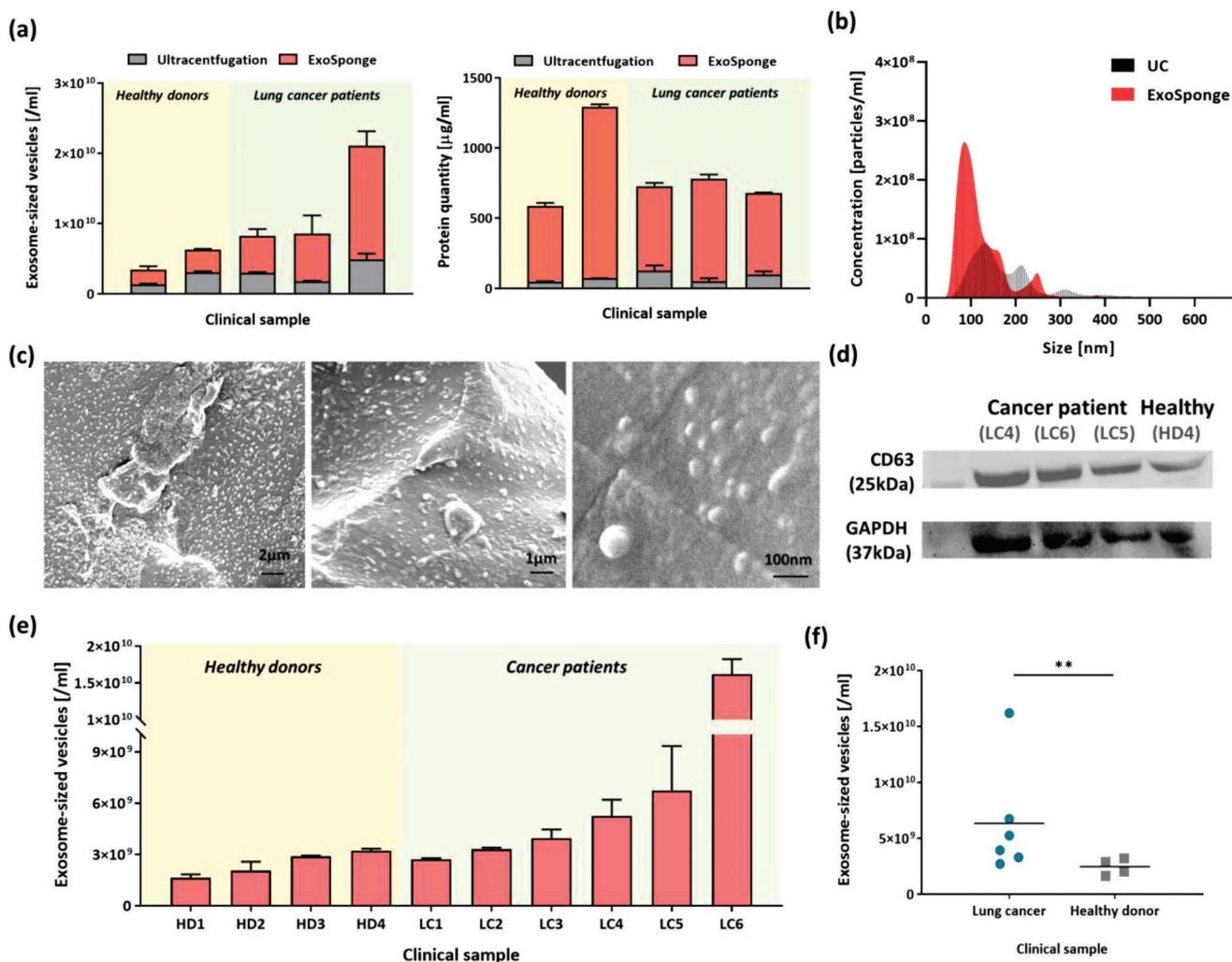
Figure 5. Clinical utility of ExoSponge (Av) platform in recovering intact extracellular vesicles (EVs) and analyzing EVs for quantitative/qualitative studies: a) EV isolation performance comparison in terms of exosome-sized vesicle concentration (left) and total protein quantity (right); b) nanoparticle tracking analysis of resultants from ExoSponge and UC; c) scanning electron microscopic analysis of isolated EVs on ExoSponge platform; d) western blot analysis of ExoSponge resultant samples; e) exosome isolation from healthy donors and cancer patients using ExoSponge; f) exosome-sized vesicle concentration comparison between two groups (line at mean value).

for cancer-derived EVs which may explain the higher isolation for the cancer patient samples.[24] This high recovery of exosomal EVs demonstrates the efficacy of ExoSponge in isolating EVs of interest for clinical use.

2.7. Exosomal Metabolites Analysis using Mass Spectrometry

The utility of serum and urinary metabolites as biomarkers for diseases has been well-established. More recently, with the discovery of metabolic cargo in exosomes,[26] the potential of exosomal metabolomics for discovering biomarkers has been more broadly recognized. Metabolomics profiling of intraexosomal cargo can prove to be a strong reflection of intratumoral metabolism that is unaffected by systemic metabolism and circulating metabolites. In this study, to this end, we extracted intraexosomal metabolites directly from exosomes adsorbed on the ExoSponge conjugated with Annexin V and anti-CD63. The

high yield efficiency of the ExoSponge and in situ extraction of metabolites from captured exosomes, coupled with the highly sensitive SCIEX 7500 UPLC-MS/MS allowed detection of metabolites in exosomes isolated less than 1 mL of blood plasma. Moreover, the ability to isolate and extract metabolites on the ExoSponge minimized the metabolite degradation and loss due to residual enzymatic activity and long procedures throughout the ultracentrifugation isolation and extraction steps.

The metabolite extracts were then profiled for polar metabolites using an LC-MS/MS workflow that covers over 500 multiple reaction monitoring (MRMs) corresponding to approximately 400 unique compounds. After performing requisite quality checks (Experimental Section), from a data set using ExoSponge conjugated with Annexin V, we detected 90 MRMs corresponding to 68 metabolites across the sample set, demonstrating an overall distinct profile of exosomal cargo in lung cancer patients compared to healthy subjects (**Figure 6**a). From a data set using ExoSponge conjugated with anti-CD63,

**ADVANCED
SCIENCE NEWS**
www.advancedsciencenews.com

**ADVANCED
MATERIALS
TECHNOLOGIES**
www.advmattechnol.de

there were intra-group variations between cancer and healthy groups and they were not statistically significant. One-factor statistical analysis revealed that 36 of 68 metabolites extracted from ExoSponge (Av) displayed large differences (fold-change > 2 or < 2-1) in intraexosomal levels in lung cancer-derived exosomes compared to exosomes in healthy subjects (Figure 6b). However, only one metabolite, phenylacetylglutamine (PAG) was statistically significantly higher in lung cancer-derived exosomes compared to healthy controls (Figure 6c). This indicates that the intraexosomal PAG level is a potential biomarker for lung cancer. High levels of PAG are found in the urine of patients with disruption in nitrogen metabolism due to hyperammonemia, urea cycle disorders, cardiovascular disease, and cancer.[35–38] PAG is synthesized in the liver and filtered out through the kidneys as a mechanism of ammonia clearance, but also produced by the gut microbiome.[37,39] Interestingly, metabolite set enrichment analysis (MSEA) in reference to metabolic signatures of diseases available in MetaboAnalyst (Experimental Section), revealed enrichment of biomarkers for phenylketonuria, cachexia in cancer patients, methylmalonic aciduria (Figure 6d,e and Table S2, Supporting Information). Interestingly, we observed levels of betaine and choline trended higher in cancer-derived exosomes (Figure 6f), which along with PAG have been described as biomarkers for prostate cancer risk.[38] Further, we also noticed remarkably high levels of methylmalonate (MMA) in two of the cancer-derived exosome samples (Figure 6g). Interestingly, age-related accumulation of intracellular MMA has been found to be a mediator for tumor progression through SOX4.[40] The capture of exosomes and extraction of intraexosomal metabolites with the ExoSponge (Av) is a novel avenue for discovering tumorigenic biomarkers that reflect intratumoral metabolism. Despite the heterogeneity we see in the metabolic profile of cancer-derived exosomes, our data strongly indicate that their metabolic cargo is distinct from that of exosomes in healthy subjects.

3. Conclusion

Due to the stability of their lipid bilayer, EVs have been emerging as a viable biomarker in many diseases including cancer and neurodegenerative diseases. However, the research has been hampered by easy access to specific EV isolation methods than can handle wide ranges of volumes. We provide an inexpensive, easily fabricated PDMS device, ExoSponge. We demonstrated that we could further modify the micro pores and make the device bio-functional for specific capture of exosomes. This efficient isolation and quick characterization analysis can lead to point-of-care cancer diagnoses. The ExoSponge device outperformed UC in total exosome isolation while maintaining purity for these bulk samples in both clinical and model samples. Annexin V-conjugated ExoSponge effectively isolated exosomes from healthy and cancer patients. The simplicity of fabrication, the rapid sampling ability, and the functionalization versatility of porous PDMS makes it a promising topic of further exploration in its application in exosome isolation as well as other medical and biological biomarker detection. Since ExoSponge inherits the adaptable conjugation properties of PDMS while adding more flexibility in target-capturing molecules and a

higher surface area, it could serve as an effective affinity-based platform for other biomolecule isolation from bulk solutions. Importantly, in addition to discovering metabolic biomarkers, intraexosomal cargo can reflect the metabolic reprogramming such as urea cycle disruption or upregulated propionate metabolism in the originating cancer cells, which demonstrates the potential value of ExoSponge (Av) as a tool for accessible, non-invasive cancer diagnostics.

4. Experimental Section

Porous PDMS Fabrication: To prepare the porous PDMS blocks, a sugar cube was utilized as the scaffolding material.[41,42] First, 1.5 × 1.5 × 1.5 cm sized sugar cubes (Domino, United States) were placed in a destructible flat weigh boat. The PDMS pre-polymer and PDMS curing agent mix (10:1) were poured over the sugar cubes until the level of the resin was equal to that of the cubes. To facilitate the adsorption of the resin into the pores of the cubes, the sugar-PDMS container was placed into a vacuum chamber for 10 min. After more PDMS mixture was added to keep the resin level above the cube, the sugar-PDMS mixture was returned to the vacuum chamber for another 40 min. Lastly, the sugar-PDMS mixture was placed in a 68 °C convection oven overnight to allow the devices to cure.

The cured sugar-PDMS composite was extracted from the container and the individual cubes were cut out, carefully making sure each side of the cubes have the sugar exposed. To dissolve the sugar from the composite, the cut-out sugar-PDMS cubes were placed in a beaker of water at 90 °C for 1–2 h with stir rods. The water was swapped out after 30 min to avoid the water from becoming saturated. To remove the remaining sugar, the cubes were placed in a beaker of 70% ethanol overnight. Lastly, the resulting cube-shaped devices were squeezed out to remove any absorbed liquid and placed into a storage container until functionalization.

The porosity was determined by first measuring the approximate volume using a ruler. Then by taking the mass of the device, its density was determined. The calculation used the known densities of air and PDMS to calculate the air mass fraction of the device.

Porous PDMS Surface Modification: For the device surface modification, it was first subjected to a piranha solution that contains sulfuric acid and hydrogen peroxide (3:1) for 10 min to transform the PDMS's natural hydrophobic and oleophobic properties into a more hydrophilic surface.[43] This oxidizing transformation allowed for the adsorption of aqueous, biological samples such as plasma, urine, and saliva. While the bath allows for sufficient oxidation of the surface, it also roughened the surface of the device which increased the surface area without affecting its ability to be further functionalized.[33,34] The surface was then conjugated following previous standard avidin-biotin chemistry[13,24] with optimization. Briefly, PDMS cubes were immersed in silane solution and incubated for an hour. The cubes were then immersed and washed with ethanol. Next, the cubes were immersed into a GMBS mixture and incubated for 30 min. After further washing with ethanol, the cubes were submerged into a NeutrAvidin solution in a conical tube and incubated overnight in a standard refrigerator. On the day of the experiment, the cubes were defrosted and washed out with filtered PBS. The coverage of NeutrAvidin in the cubes was evaluated and confirmed using biotinylated staining dye. The PBS wash was followed by the conjugation of EV binding protein, Annexin V or anti-CD63. The cubes for experiments were soaked into biotinylated Annexin V solution (50 μL Annexin V + 1 mL of 1 × binding buffer) or anti-CD63 (20 μL Anti-CD63+ 1 mL PBS) and incubated for 40 min.

Cancer Cell Culture and Exosome Sample Preparation: H3255 lung cancer cell culture supernatant was used throughout this study. Cell lines were cultured in Dulbecco's modified Eagle's minimal essential media (DMEM, Life Technologies, Inc.). Media was supplemented with 10% (v/v) exosome-depleted fetal bovine serum (System Bioscience, LLC) and 1% (v/v) penicillin–streptomycin (Invitrogen).
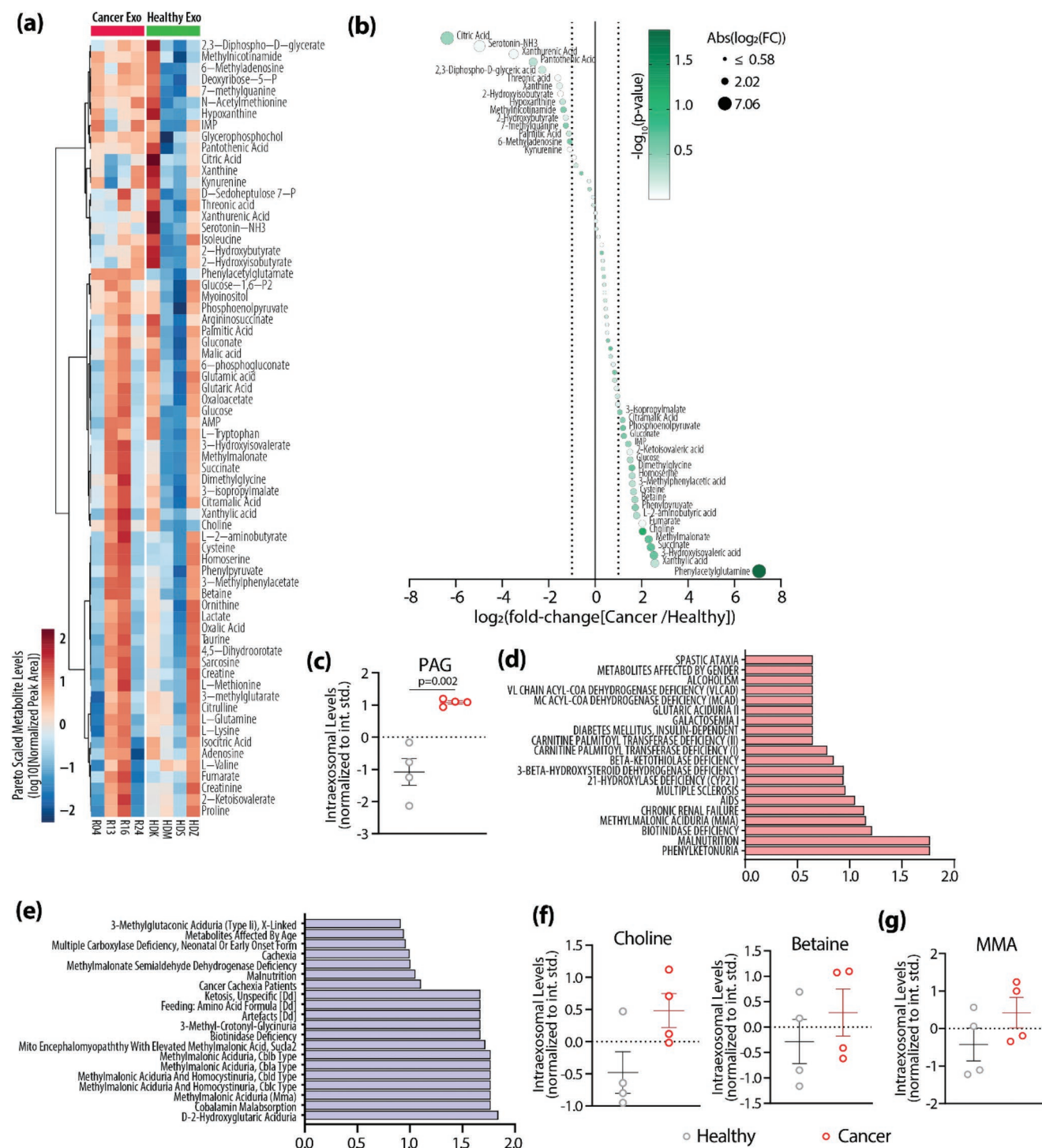
Figure 6. Analysis of exosomal metabolites isolated using ExoSponge conjugated with Annexin V: a) Heatmap of intraexosomal metabolite levels detected by LC-MS/MS in cancer-derived exosomes (red) compared to exosomes from healthy subjects (green); b) Waterfall plot demonstrating differentially abundant intraexosomal metabolites from cancer patient-derived samples compared to healthy subjects; c) intraexosomal metabolite level of phenylacetylglutamine; d) MSEA showing top 20 metabolite sets representing disease signatures in plasma metabolites, enriched in exosomes from cancer patients compared to healthy subjects; e) MSEA showing top 20 metabolite sets representing disease signatures in urine metabolites, enriched in exosomes from cancer patients compared to healthy subjects; f) intraexosomal metabolite level of betaine and choline; g) intraexosomal metabolite level of methylmalonate. Metabolite levels were analyzed using MetaboAnalyst 5.0 after normalizing metabolite signals to sample-specific internal standard, mean-centered, and Pareto-scaled.

For the exosome model samples, a count of 1×10^5 cancer cells was incubated in exosome-depleted media for 1 day, then cell culture supernatant (CCS) was gently replaced from the cell plate. This CCS was followed by mild centrifugation for excess cell or bigger aggregation elimination, and then 1–3 ml of CCS was prepared for model sample studies.

The sample collection and experiments were approved by the University of Michigan Institutional Review Board (IRB). Informed consent was obtained from all participants of this clinical study and non-small cell lung cancer blood samples were gathered after approval of the institutional review board at the University of Michigan (HUM00119934). Blood samples were centrifuged at 1000xg for 10 min to isolate and extract plasma from the blood. The plasma extract was further diluted with 10x binding buffer (10:1) for exosome isolation.

EV Isolation/Release using ExoSponge: For sample processing, two ExoSponge devices were used for 5 ml of the sample containing plasma or model exosomes (2.5 ml per device). Samples were either prepared in the 1x of binding buffer containing 2.5 mM of $CaCl_2$ to be actively conjugated with Annexin V (Cat #: BD 556417, BD Biosciences, USA) or 1x PBS buffer solution for anti-CD63-based experiments (Cat #: 215030, Ancell Corporation, USA). Before exosome isolation occurs, a 10x binding buffer was added to the biological sample at a 10 to 1 respective ratio of sample to buffer. Cell supernatant samples were incubated for 20 to 60 min. After incubation at room temperature, the cubes were removed and washed with a 1x binding buffer solution. To release the affinity between Annexin V and the EVs, 10 mM EDTA was added to the device. The chelating agent targeted divalent metal ions which removed the necessary calcium ions. Afterward, the isolated sample was squeezed out of the device. The resulting volume absorbed from one ExoSponge ranged from 1.4 to 1.9 ml and the exosomal concentration was further normalized using this volume. All samples conjugated with Anti-CD63 protein were washed and prepared with the same procedures but using only filtered PBS instead of binding buffer solution.

EV Isolation/Release using Ultracentrifugation: Ultracentrifugation was used to prepare an exosome model sample and comparison studies. In both cases, a Sorvall ultracentrifuge (ThermoFisher, USA) was used. For comparison study, the same volume of initial plasma/cell culture supernatant sample was used but diluted into an equal amount of filtered buffer solution. Plasma/cell culture supernatant samples were first centrifuged at 2000 g for 15 min, and then 12 000 g for 20 min to remove cellular debris. After initial ultracentrifugation at 100 000 g for 90 min, the supernatant was aspirated, and another 38 mL of PBS was injected for a second round of ultracentrifugation at the same conditions. The pellet after the second UC was gently spiked into buffer solution at the same volume as the ExoSponge resultant solution.

Scanning Electron Microscopy (SEM) Analysis: In preparation for SEM imaging, the EV-containing device was treated with 2% glutaraldehyde to retain the morphology, for 1 h while on ice. After being rinsed with PBS, the samples were subjected to bath concentrations of ethanol (50%, 70%, 90%, 95%, and 100%) for 10 min each (two times for 100%) to dehydrate the samples. Afterward, hexamethyldisilazane (HMDS) (Emsdiasum, United States) was used to dry the samples preceding an overnight air drying in the hood. The dehydrated samples were mounted on aluminum stubs using both carbon tape and glue, then sputter-coated with gold particles to form a conductive layer. The TESCAN RISE SEM at the Michigan Center for Materials Characterization (MC²) at the University of Michigan was utilized for surface imagining.

EV Recovery Evaluation using Nanoparticle Tracking Analysis: After EDTA treatment and sample extraction outlined in Section 2.4, the sample was taken for NTA using NanoSight NS300 (Malvern Instruments, UK). This process was used to quantify the concentrations and size distribution of the recovered samples from ExoSponge devices. 30 µL of the resultant was used and a laser module was mounted inside the main instrument housing. Based on the Brownian motion of nanoparticles, this equipment visualized the scattered lights from the particles of interest. This movement was monitored through a video sequence for 20 s in triplicate. All data acquisition and processing were performed using NanoSight NS300 control software. After the particle data was recorded based on

their size, the area of interest, between 30 and 150 nm, was analyzed for exosomal concentration as well as total vesicle concentration.

Protein Quantity Evaluation using Micro-BCA Analysis: EV lyses were acquired using radio-immunoprecipitation assay (RIPA) buffer (Cat #: 89900, ThermoFisher Scientific, USA) with 1% protease inhibitor (Cat#: 78441, ThermoFisher Scientific, USA). The prepared buffer solution was applied to ExoSponge after exosome isolation and washing steps. ExoSponge devices were incubated with RIPA buffer for 10 min in a conical tube and followed by mild centrifugation to collect the supernatant. Incubated RIPA buffer was collected for micro-BCA analysis and incubated with working buffer, as per the manufacturer's instructions, for 2 h in 37 °C wrapped in aluminum foil. The total protein amount was measured with the Synergy NEO HTS Multi-Mode Reader (Agilent, United States) and by extrapolation through a standard curve generated as per the manufacturer's instructions.

Protein Identification using Western Blot Analysis: Isolated ExoSponge EV protein lysate was prepared using RIPA buffer (Cat #: 89900, ThermoFisher Scientific, USA) with 1% protease inhibitor (Cat#: 78441, ThermoFisher Scientific, USA). Sample preparation was conducted by mixing 37.5 µL of ExoSponge lysate with 12.5 µL of working buffer (10:1 of Laemmli and 2-mercaptoethanol, respectively) for a 50 µL sample solution. Protein samples were boiled for 7 min, then cooled on ice, and subjected to SDS-PAGE. The proteins were transferred onto polyvinylidene difluoride (PVDF) membranes (Cat#: 1620261, Bio-Rad Laboratories, USA) using a semi-dry Trans-Blot Turbo system (Bio-Rad Laboratories, USA). Blots were incubated in EveryBlot blocking buffer (Cat#: 12010020, Bio-Rad Laboratories, USA) for 5 min at room temperature and then with their respective primary antibodies (anti-CD63 and anti-GAPDH, Santa Cruz Biotechnology, USA) diluted in TBST (containing 0.1% Sodium azide) overnight at 4 °C. Afterwards, blots were washed with TBST and incubated with anti-rabbit HRP secondary antibodies (Millipore Sigma, USA) in 5% Blotting-Grade Blocker (Cat#: 1706404, Bio-Rad Technologies, USA) and detected using SuperSignal West Pico Chemiluminescent Substrate (Thermo Scientific, USA) and ChemiDoc Imaging System (Bio-Rad Technologies, USA).

Clinical Sample Preparation and Processing: In preparation for ExoSponge isolation, 10 mL of plasma sample was combined with 1 mL of 10x binding buffer solution containing 25 mM of $CaCl_2$. (BD Bioscience, USA). Each cube device was placed in a solution volume of 1.5 mL and each one was incubated for 40 min at room temperature. For each of the five clinical samples, a group for NTA and micro-BCA analysis was prepared. ExoSponge samples going to NTA and protein analysis were subjected to 1 mL of 10 mM EDTA treatment with the samples going to BCA and western blotting analysis, also having a 500 µL solution of 1 mL of RIPA lysis buffer and 10 µL of PIC was added. At the same time, equal amounts of sample solution were saved and underwent UC for further performance comparison study.

Exosomal Metabolite Extraction for Mass Spectrometry: To facilitate metabolite extraction, 750 µL of Optima methanol (Cat#: A454-1, ThermoFisher Scientific, USA) at −20 °C and 750 µL of Optima water (Cat #: W71, ThermoFisher Scientific, USA) containing 0.5 µg of norvaline internal standard as well mixed with ExoSponge-bound exosomes. The solution was squeezed out from the ExoSponge and centrifuged at 4000 rpm for 3 min to remove debris. The supernatant was combined with an equal volume of chloroform at −20 °C and then vortexed at 4 °C for 15 min. The mixed solution was centrifuged at 17 000xg and 4 °C for 10 min to separate into three layers. The upper polar layer of methanol and water containing polar metabolites was pipetted off into a new tube and dried via vacuum centrifugation. The polar metabolites were then resuspended in 50% methanol for LC-MS/MS injection.

Metabolomics Analysis: The samples were analyzed with SCIEX Triple QuadTM 7500 LC-MS/MS QTRAP coupled to the ExionLCTM system. A scheduled MRM MS method was set up using the following parameters: GS1 = 45 psi, GS2 = 70 psi, spray voltage = 1600 V, temperature = 450 °C, settling time = 15 ms, and pause time = 3 ms. The LC method was adapted from a global metabolomics protocol provided by SCIEX. Briefly, the analytes were separated using Phenomenex's Kinetex, 2.6 µM F5 100 A (150 ×2.1 mm) equipped with SecurityGuard ULTRA Cartridge. Mobile

**ADVANCED
SCIENCE NEWS**

www.advancedsciencenews.com

**ADVANCED
MATERIALS
TECHNOLOGIES**

www.advmattechnol.de

phase A was 0.1% formic acid in water while mobile phase B was 0.1% formic acid in acetonitrile. Analysis time was 20 min with the following gradient: 0 min 0% B, 2.1 min 0% B, 14 min 95% B, 16 min 95% B, 16.1 min 0% B. and finally 20 min 0% B. Column temperature was set at 30 °C. The flow rate was 0.2 mL min^{-1} and 1–5 µL of each sample was injected per run. Peaks were extracted and integrated by SCIEX OS 2.0, after filtering for good-quality peaks. Peak quality was estimated by SCIEX OS-based on peak height, width at half-height, signal-to-noise ratio, and retention time-shift. Finally, software-assigned good-quality peaks were checked visually and filtered further. Peak areas of all metabolites were normalized to the volume of plasma used to isolate exosomes and the peak area for the internal standard, norvaline. Further, analysis was performed with MetaboAnalyst 5.0. One-factor statistical analysis was used for estimating fold-change and multiple hypotheses testing. Enrichment analysis was used to identify metabolite-associated disease signatures from the blood and urine biomarker sets available in the MetaboAnalyst 5.0 knowledge base.

Statistical Analysis: All results present as mean ± standard deviation. Statistical analysis was demonstrated using Prism software. Unpaired *t*-tests (two-tailed) were used to compare the differences in exosome-sized vesicle concentration between lung cancer patients ($n = 6$) versus healthy controls ($n = 4$). Statistical significance was defined as a two-tailored $p < 0.05$. For metabolomics analysis, One-factor statistical analysis was used for estimating fold-change and multiple hypotheses testing.

Supporting Information

Supporting Information is available from the Wiley Online Library or from the author.

Acknowledgements

Conflict of Interest

The authors declare no conflict of interest.

Data Availability Statement

The data that support the findings of this study are available from the corresponding author upon reasonable request.

Keywords

circulating biomarkers, extracellular vesicles, liquid biopsy, microsystems, polydimethylsiloxane sponges, porous polydimethylsiloxane

[1] M. Simons, G. Raposo, *Curr. Opin. Cell Biol.* **2009**, *21*, 575.
[2] T. L. Whiteside, *Adv. Clin. Chem.* **2016**, *74*, 103.
[3] R. E. Lane, D. Korbie, M. M. Hill, M. Trau, *Clin. Transl. Med.* **2018**, *7*, 14.
[4] D. Hanahan, R. A. Weinberg, *Cell* **2011**, *144*, 646.
[5] N. Ludwig, T. L. Whiteside, T. E. Reichert, *Int. J. Mol. Sci.* **2019**, *20*, 4684.
[6] Z. Niu, R. T. K. Pang, W. Liu, Q. Li, R. Cheng, W. S. B. Yeung, *PLoS One* **2017**, *12*, 0186534.
[7] E. Multia, C. J. Y. Tear, M. Palviainen, P. Siljander, M.-L. Riekkola, *Anal. Chim. Acta* **2019**, *1091*, 160.
[8] E. Multia, T. Liangsupree, M. Jussila, J. Ruiz-Jimenez, M. Kemell, M.-L. Riekkola, *Anal. Chem.* **2020**, *92*, 13058.
[9] P. Zhang, M. He, Y. Zeng, *Lab Chip* **2016**, *16*, 3033.
[10] Y.-T. Kang, Y. J. Kim, J. Bu, Y.-H.o Cho, S.-W. Han, B.-I.n Moon, *Nanoscale* **2017**, *9*, 13495.
[11] K. Lee, H. Shao, R. Weissleder, H. Lee, *ACS Nano* **2015**, *9*, 2321.
[12] F. Liu, O. Vermesh, V. Mani, T. J. Ge, S. J. Madsen, A. Sabour, E.n-C. Hsu, G. Gowrishankar, M. Kanada, J. V. Jokerst, R. G. Sierra, E. Chang, K. Lau, K. Sridhar, A. Bermudez, S. J. Pitteri, T. Stoyanova, R. Sinclair, V. S. Nair, S. S. Gambhir, U. Demirci, *ACS Nano* **2017**, *11*, 10712.
[13] Y.-T. Kang, Y. J. Kim, B. Rupp, E. Purcell, T. Hadlock, N. Ramnath, S. Nagrath, *Anal. Sens.* **2021**, *1*, 117.
[14] K. Raj M, S. Chakraborty, *J. Appl. Polym. Sci.* **2020**, *137*, 48958.
[15] T. Fujii, *Microelectron. Eng.* **2002**, *61–62*, 907.
[16] K. Takeuchi, N. Takama, R. Kinoshita, T. Okitsu, B. Kim, *Biomed. Microdevices* **2020**, *22*, 79.
[17] Q.i Li, T. Duan, J. Shao, H. Yu, *J. Med. Aromat. Plant Sci.* **2018**, *53*, 11873.
[18] S. Masihi, M. Panahi, D. Maddipatla, A. J. Hanson, A. K. Bose, S. Hajian, V. Palaniappan, B. B. Narakathu, B. J. Bazuin, M. Z. Atashbar, *ACS Sens.* **2021**, *6*, 938.
[19] C. Yu, C. Yu, L. Cui, Z. Song, X. Zhao, Y. Ma, L. Jiang, *Adv. Mater. Interfaces* **2016**, *4*, 1600862.
[20] A. Norfatriah, A. S. Ahmad Syamaizar, A. S. Zuruzi, *IOP Conf. Ser.: Mater. Sci. Eng.* **2018**, *342*, 012050.
[21] S. Yoon, M. Seok, M. Kim, Y.-H. Cho, *Sci. Rep.* **2021**, *11*, 938.
[22] M. G. King, A. J. Baragwanath, M. C. Rosamond, D. Wood, A. J. Gallant, *Procedia Chem.* **2009**, *1,*, 568.
[23] J. Suthar, E. S. Parsons, B. W. Hoogenboom, G. R. Williams, S. Guldin, *Anal. Chem.* **2020**, *92*, 4082.
[24] Y.-T. Kang, E. Purcell, C. Palacios-Rolston, T.-W. Lo, N. Ramnath, S. Jolly, S. Nagrath, *Small* **2019**, *15*, 1903600.
[25] A. Achreja, N. Meurs, D. Nagrath, *Metabolic Flux Analysis in Eukaryotic Cells, Methods in Molecular Biology*, Vol. *2088*, Humana Press, New York **2020**.
[26] H. Zhao, L. Yang, J. Baddour, A. Achreja, V. Bernard, T. Moss, J. C. Marini, T. Tudawe, E. G. Seviour, F. A. San Lucas, H. Alvarez, S. Gupta, S. N. Maiti, L. Cooper, D. Peehl, P. T. Ram, A. Maitra, D. Nagrath, *Elife* **2016**, *5*, 10250.
[27] S. R. Kumar, E. T. Kimchi, Y. Manjunath, S. Gajagowni, A. J. Stuckel, J. T. Kaifi, *Sci. Rep.* **2020**, *10*, 2800.
[28] A. Achreja, H. Zhao, L. Yang, T. H. Yun, J. Marini, D. Nagrath, *Metab. Eng.* **2017**, *43*, 156.
[29] H. Zhao, A. Achreja, E. Iessi, M. Logozzi, D. Mizzoni, R. Di Raimo, D. Nagrath, S. Fais, *Biochim. Biophys. Acta, Rev. Cancer* **2018**, *1869*, 64.
[30] Y. Du, L. Chen, X.-S. Li, X.-L. Li, X.-D. Xu, S.-B. Tai, G.-L. Yang, Q. Tang, H. Liu, S.-H. Liu, S.-Y. Zhang, Y. Cheng, *Schizophr. Bull.* **2021**, *47*, 615.
[31] L. Tao, J. Zhou, C. Yuan, L. Zhang, D. Li, D. Si, D. Xiu, L. Zhong, *Metabolomics* **2019**, *15*, 86.
[32] A. Zebrowska, A. Skowronek, A. Wojakowska, P. Widlak, M. Pietrowska, *Int. J. Mol. Sci.* **2019**, *20*, 3461.
[33] L. Zhang, Q. Li, R. Yang, Z. Xu, Y. Kang, P. Xue, *Biomed. Microdevices* **2019**, *21*, 58.

[34] W. Chen, S. Weng, F. Zhang, S. Allen, X. Li, L. Bao, R. H. W. Lam, J. A. Macoska, S. D. Merajver, J. Fu, *ACS Nano* **2013**, *7*, 566.

[35] M. Mokhtarani, G. A. Diaz, W. Rhead, U. Lichter-Konecki, J. Bartley, A. Feigenbaum, N. Longo, W. Berquist, S. A. Berry, R. Gallagher, D. Bartholomew, C. O. Harding, M. S. Korson, S. E. Mccandless, W. Smith, J. Vockley, S. Bart, D. Kronn, R. Zori, S. Cederbaum, N. Dorrani, J. L. Merritt, S. Sreenath-Nagamani, M. Summar, C. Lemons, K. Dickinson, D. F. Coakley, T. L. Moors, B. Lee, B. F. Scharschmidt, *Mol. Genet. Metab.* **2012**, *107*, 308.

[36] M. C. Machado, F. Pinheiro Da Silva, *J. Intensive Care* **2014**, *2*, 22.

[37] I. Nemet, P. P. Saha, N. Gupta, W. Zhu, K. A. Romano, S. M. Skye, T. Cajka, M. L. Mohan, L. Li, Y. Wu, M. Funabashi, A. E. Ramer-Tait, S. V. Naga Prasad, O. Fiehn, F. E. Rey, W. H. W. Tang, M. A. Fischbach, J. A. Didonato, S. L. Hazen, *Cell* **2020**, *180*, 862.

[38] C. A. Reichard, B. D. Naelitz, Z. Wang, X. Jia, J. Li, M. J. Stampfer, E. A. Klein, S. L. Hazen, N. Sharifi, *Cancer Epidemiol., Biomarkers Prev.* **2022**, *31*, 192.

[39] J. S. Lee, L. Adler, H. Karathia, N. Carmel, S. Rabinovich, N. Auslander, R. Keshet, N. Stettner, A. Silberman, L. Agemy, D. Helbling, R. Eilam, Q. Sun, A. Brandis, S. Malitsky, M. Itkin, H. Weiss, S. Pinto, S. Kalaora, R. Levy, E. Barnea, A. Admon, D. Dimmock, N. Stern-Ginossar, A. Scherz, S. C. S. Nagamani, M. Unda, D. M. Wilson, R. Elhasid, A. Carracedo, et al., *Cell* **2018**, *174*, 1559.

[40] A. P. Gomes, D. Ilter, V. Low, J. E. Endress, J. Fernández-García, A. Rosenzweig, T. Schild, D. Broekaert, A. Ahmed, M. Planque, I. Elia, J. Han, C. Kinzig, E. Mullarky, A. P. Mutvei, J. Asara, R. De Cabo, L. C. Cantley, N. Dephoure, S.-M. Fendt, J. Blenis, *Nature* **2020**, *585*, 283.

[41] M. Amjadi, M. S. Kim, I. Park, *in 14th IEEE Int. Conf. on Nanotechnology*, IEEE, Toronto, Canada **2014**, p. 764–767.

[42] L.i-W. Lo, J. Zhao, H. Wan, Y. Wang, S. Chakrabartty, C. Wang, *ACS Appl. Mater. Interfaces.* **2022**, *14*, 9570.

[43] Y. J. Kim, Y.-T. Kang, Y.-H. Cho, *Anal. Chem.* **2016**, *88*, 7938.